Rainer Grün
Research School of Earth Sciences, Australian National University, Canberra ACT 0200, Australia. E-mail: rainer.grun@anu.edu.au

Peter Beaumont
McGregor Museum, Kimberley, South Africa. E-mail: archaeol@kimberley.co.za

Received 17 November 1999
Revision received 17 January 2001 and accepted 23 February 2001

Keywords: Border Cave, Howieson's Poort, MSA, LSA, ESR dating, BC1 to BC8.

Border Cave revisited: a revised ESR chronology

In view of a decade of progress in ESR dating we have revised the ESR chronology of Border Cave. A detailed gamma ray survey in 1994 and newly calculated beta attenuation data led to total dose rate estimations that are between 0 and 30% smaller than previously estimated. Accordingly, the resulting ESR age estimates are between 0 and 30% older. The ESR dates are now in good agreement with independent age estimates, particularly ^{14}C and amino acid racemization. New ESR dates for the lowermost dated sedimentary layer, 5 WA (white ash), indicate that the sedimentation of the sequence started around 200 ka ago.

Journal of Human Evolution (2001) **40,** 467–482
doi:10.1006/jhev.2001.0471
Available online at http://www.idealibrary.com on IDEAL®

Introduction

In 1990 we published a detailed ESR chronology on tooth enamel samples recovered from the sedimentary sequence at Border Cave (Grün *et al.*, 1990). Although ranging between 28 and 140 ka, the results were disputed because the ESR data were somewhat younger than expected (e.g., Miller & Beaumont, 1989).

There are a number of reasons for re-assessing the 1990 data. First of all, the dataset represents the most detailed ESR sequence published so far. Furthermore, the site is ideally suited for ESR dating, because no samples contain significant amounts of uranium. Thus, differences caused by modelling U-uptake are virtually negligible (for details on ESR age modelling see Grün, 1989). Border Cave is therefore an ideal test case for ESR dating. Figure 1 shows a site plan of the archaeological excavations.

Since 1990, the following has changed in ESR data evaluation:

(1) The fitting of the dose–response curve is now carried out with a more appropriate algorithm and errors are calculated with an analytical method (Brumby, 1992). The data points are weighted inversely proportional to the ESR intensity. These procedures were confirmed to be appropriate by computer simulation (Grün & Brumby, 1994) and reproducibility tests (Grün, 1998*a*). The previously applied fitting procedures, which are based on equal weights and jack-knifing error calculation (Grün & Macdonald, 1989), lead to marginally different dose estimations (usually within a few percent, see below) but to errors which are much too large (Grün & Brumby, 1994). It was not possible to use the spectra for more sophisticated spectrum analysis,

0047–2484/01/060467+16 $35.00/0

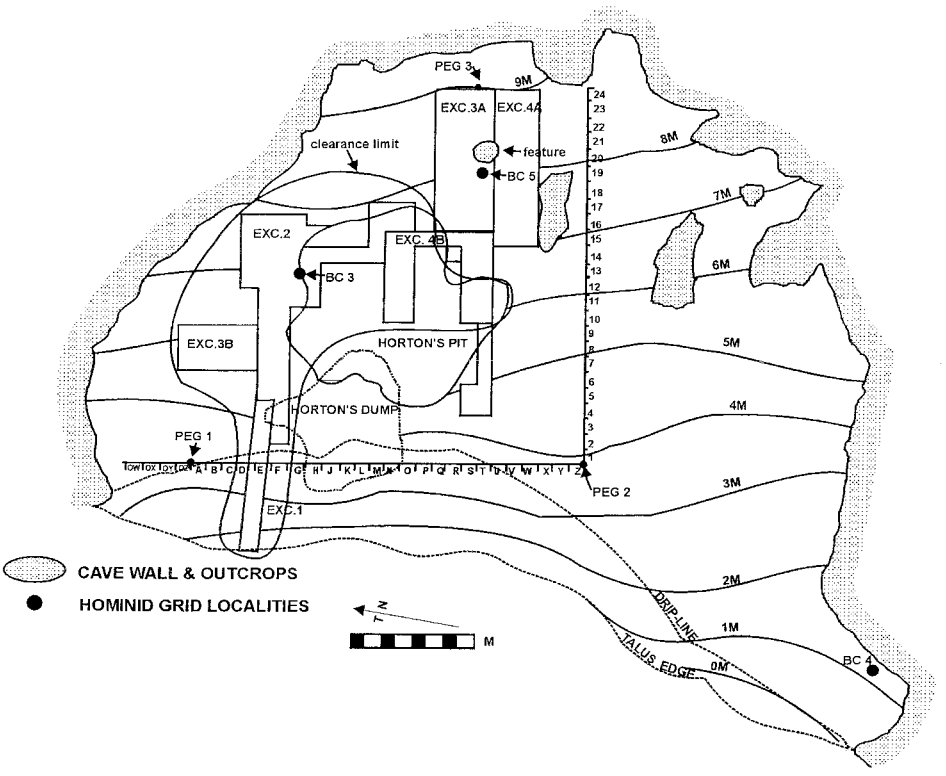

Figure 1. A plan of Border Cave showing the extent of the clearance in 1987, the location of Excavations 1 to 4, and the grid localities of hominids BC3 to BC5.

e.g., deconvolution (Grün, 1998*b*) or maximum likelihood common factor analysis (Vanhaelewyn *et al.*, 2000), because at the time of measurement, the ESR spectrometer was not equipped with digital data recording. However, a comparison of different methods of dose evaluation shows that the peak-to-peak measurements used in this study yield, in most cases, statistically indistinguishable results from more computing intensive methods (Grün, 2000*a*, 2001*b*).

(2) The gamma dose rate was measured in 1988 at only a few places in the cave. The dose rates for some layers were obtained by interpolation. In 1994, we carried out a detailed gamma survey of the cave. It showed that the earlier measurements were reproduced but some layers have a more complex gamma ray distribution than originally supposed.

(3) In 1997, Yang carried out experiments for assessing beta attenuation factors. These new factors are in very good agreement with calculations based on One Group Theory as well as Monte Carlo simulations (see also Brennan *et al.*, 1997, 2000; Yang *et al.*, 1998). The main implication for ESR dating is that the new attenuation factors are significantly smaller than those experimentally determined by Aitken *et al.* (1985) and calculated by Grün (1986).

(4) In 1998, Adamiec & Aitken published new dose rate values for radioisotopes which are slightly different from those of Nambi & Aitken (1986).

For further details of ESR dating see recent reviews by Ikeya (1993), Grün (1997, 2000*b*,*c*,*d*, 2001*a*) and Rink (1997).

Results

The analytical details of the re-assessment of the ESR chronology of Border Cave are given in Table 1. As mentioned above, there is virtually no difference between early U-uptake (EU) and linear U-uptake (LU) age calculations, and most differences are attributable to rounding. In this paper only the EU age estimates are further discussed.

Dose evaluation

Figure 2 shows the dose and error estimations using the two different procedures. All dose values, except for sample 603A, agree within error [Figure 2(a)]. In Figure 2(b), the errors are removed for clarity. A linear regression of the dose pairs results in virtually in a 1:1 relationship, thus, the re-evaluation of the dose values has a negligible effect on the calculated ages. Figure 2(c) compares the different error procedures. It shows that the jack-knifing errors are always larger than the errors derived from analytical expression (except for sample 603A). This is expected from the computer simulations (Grün & Brumby, 1994). Reproducibility tests have shown that the analytical expression using weights inverse proportional to the squared intensity yields errors which are most appropriate for the dose estimation using tooth enamel powder samples (Grün, 1998*a*).

Gamma dose rate

Figure 3 shows the measured gamma dose rates which tend to decrease from the back wall towards the cave mouth. This may be attributable to the fact that the number of artefacts increase in the same direction, i.e., the sedimentary composition of the layers changes. Most of the measurements were carried out in strips T to U of Excavation 3A (see Figure 1). The previous gamma measurements show exceptionally good agreement with the newer survey, although first, different equipment was used: a three-channel Harwell spectrometer in 1988, calibrated for U, Th, and K separately with a 3×3 inch NaI detector, and a multichannel Canberra Packard spectrometer in 1994 calibrated for total dose rate using a 1×2 inch CsI detector. Second, some of the earlier measurements were carried out further to the north in strips N and O.

It can be seen from Figure 3 that the gamma dose rate decreases downward from layers 1BS towards 4WA, but then starts to increase again in the layers below 4WA. Furthermore, 4WA has significantly lower dose rates at the top than at the base. For age calculation, the gamma dose rate values of a distinctive layer were fitted with a linear function and the dose rate values for a particular strip (13 to 24) were obtained by interpolation. The grid for the location of the samples is shown in Figure 1. Most of the original measurements were carried out in the back of the cave (strips 20 to 24) whilst most of the samples were collected from strips 14 to 17. Therefore, the gamma dose rate values used in the earlier calculations were somewhat too high.

Figure 4(a) shows the comparison of the gamma dose rates used in the previous age calculation and in the revised set. Particularly large deviations occur for unit 4WA and 1RGBS. Originally, no measurement was carried out in 4WA and the data from 4BS and 5BS, which are very close, were averaged to obtain the dose rate for 4WA. As mentioned above, the gamma dose rate distribution of 4WA is complex and

Table 1 Results of chemical analysis and revised ESR age estimates for samples from Border Cave

							Sediment					Early U-uptake				Linear U-uptake			
Sample no.	Square	D_E (Gy)	U (EN) (ppm)	U (DE) (ppm)	TT (μm)	S1/S2 (μm)	U (ppm)	Th (ppm)	K (%)	γ-$\dot{D}$ (μGy/a)	β-$\dot{D}$ (μGy/a)	int.$\dot{D}$ (μGy/a)	DE-$\dot{D}$ (μGy/a)	Total $\dot{D}$ (μGy/a)	Age (ka)	int.$\dot{D}$ (μGy/a)	DE-$\dot{D}$ (μGy/a)	Total $\dot{D}$ (μGy/a)	Age (ka)
										1BS LR1									
531a	W17	53·2 ± 1·3	0·01	0·01	1240	50	1·99	12	1·71	1560 ± 78	195 ± 19	2 ± 2	0 ± 0	1757 ± 80	30 ± 2	1 ± 1	0 ± 0	1756 ± 80	30 ± 2
531b		55·6 ± 0·9	0·05	0·01	1100	50	1·99	12	1·71	1560 ± 78	222 ± 23	10 ± 2	0 ± 0	1792 ± 81	31 ± 1	4 ± 2	0 ± 0	1786 ± 81	31 ± 1
531c*		53·0 ± 0·9	0·01	0·01/0·01	1100	50	1·99	12	1·71	1560 ± 78	0 ± 0	2 ± 2	0 ± 0	1562 ± 78	34 ± 2	1 ± 1	0 ± 0	1561 ± 78	34 ± 2
644a	W15	64·1 ± 1·7	0·01	0·01	850	50	1·67	8·1	1·46	1560 ± 78	234 ± 26	2 ± 2	0 ± 0	1796 ± 82	36 ± 2	1 ± 1	0 ± 0	1795 ± 82	36 ± 2
644b		69·5 ± 4·6	0·01	0·01	800	50	1·67	8·1	1·46	1560 ± 78	247 ± 28	2 ± 2	0 ± 0	1809 ± 83	38 ± 3	1 ± 1	0 ± 0	1808 ± 83	38 ± 3
646a	W16	61·0 ± 1·6	0·01	0·01	1100	50	1·95	8·8	1·53	1560 ± 78	195 ± 20	2 ± 2	0 ± 0	1757 ± 80	35 ± 2	1 ± 1	0 ± 0	1756 ± 80	35 ± 2
646b		66·1 ± 3·0	0·01	0·01	900	50	1·95	8·8	1·53	1560 ± 78	238 ± 26	2 ± 2	0 ± 0	1800 ± 82	37 ± 2	1 ± 1	0 ± 0	1799 ± 82	37 ± 2
														Average	33 ± 1				33 ± 1
										1WA. UP									
645a	R17	59·7 ± 3·1	0·01	0·01	800	50	1·89	9·1	1·83	1300 ± 100	301 ± 34	2 ± 2	0 ± 0	1603 ± 106	37 ± 3	1 ± 1	0 ± 0	1602 ± 106	37 ± 3
645b		70·9 ± 7·0	0·01	0·01	800	50	1·89	9·1	1·83	1300 ± 100	301 ± 34	2 ± 2	0 ± 0	1603 ± 106	44 ± 5	1 ± 1	0 ± 0	1602 ± 106	44 ± 5
														Average	39 ± 3				39 ± 3
										1WA 2									
530a	W19	54·4 ± 0·9	0·10	0·13	1150	50	2·09	14	1·72	1345 ± 100	220 ± 22	20 ± 4	1 ± 0	1586 ± 103	34 ± 2	9 ± 2	1 ± 1	1575 ± 102	35 ± 2
530b*		50·9 ± 0·8	0·01	0·13/0·22	1150	50	2·09	14	1·72	1345 ± 100	0 ± 0	2 ± 2	1 ± 0	1350 ± 100	38 ± 3	1 ± 1	1 ± 1	1348 ± 100	38 ± 3
530c*		56·3 ± 1·3	0·46	0·22/0·01	750	50	2·09	14	1·72	1345 ± 100	0 ± 0	94 ± 14	3 ± 1	1442 ± 101	39 ± 3	42 ± 6	1 ± 0	1388 ± 100	41 ± 3
														Average	36 ± 1				37 ± 1
										2BS. UP									
540a	T22	67·2 ± 2·3	0·01	0·01	1900	50	2·41	11	1·88	1500 ± 100	141 ± 8	2 ± 3	0 ± 0	1643 ± 100	41 ± 3	1 ± 1	0 ± 0	1642 ± 100	41 ± 3
540b		64·8 ± 3·5	0·07	0·01	2500	100	2·41	11	1·88	1500 ± 100	100 ± 6	16 ± 3	0 ± 0	1616 ± 100	40 ± 4	7 ± 2	0 ± 0	1607 ± 100	40 ± 4
														Average	41 ± 2				41 ± 2
										2BS. LR. C									
532a	S18	79·2 ± 2·7	0·01	0·04	1450	50	1·88	10·5	1·61	1425 ± 100	153 ± 14	2 ± 3	0 ± 0	1580 ± 101	50 ± 3	1 ± 1	0 ± 0	1579 ± 101	50 ± 3
532b		82·3 ± 1·9	0·11	0·16	1140	50	1·88	10·5	1·61	1425 ± 100	199 ± 21	25 ± 5	1 ± 2	1650 ± 102	50 ± 3	11 ± 2	1 ± 0	1636 ± 102	50 ± 3
532c		75·9 ± 1·6	0·01	0·08	1400	50	1·88	10·5	1·61	1425 ± 100	158 ± 14	2 ± 3	1 ± 0	1586 ± 101	48 ± 3	1 ± 1	0 ± 0	1584 ± 101	48 ± 3
533a	S18	73·8 ± 1·5	0·01	0·04	1350	50	1·88	10·5	1·61	1425 ± 100	165 ± 15	2 ± 2	0 ± 0	1592 ± 101	46 ± 3	1 ± 1	0 ± 0	1591 ± 101	46 ± 3
533b*		73·1 ± 3·5	0·01	0·01/0·01	1400	50	1·88	10·5	1·61	1425 ± 100	0 ± 0	2 ± 3	0 ± 0	1427 ± 100	51 ± 4	1 ± 1	0 ± 0	1426 ± 100	51 ± 4
537a	U17	68·2 ± 2·5	0·01	0·01	1500	50	1·36	10·0	1·35	1400 ± 100	123 ± 10	2 ± 3	0 ± 0	1525 ± 101	45 ± 3	1 ± 1	0 ± 0	1524 ± 101	45 ± 3
537b		74·6 ± 1·9	0·01	0·01	1250	50	1·36	10·0	1·35	1400 ± 100	151 ± 15	2 ± 3	0 ± 0	1553 ± 101	48 ± 3	1 ± 1	0 ± 0	1552 ± 101	48 ± 3
537c		103·7 ± 1·8	0·01	0·04	1200	50	1·36	10·0	1·35	1400 ± 100	157 ± 16	3 ± 2	0 ± 0	1560 ± 101	(66 ± 4)	1 ± 1	0 ± 0	1558 ± 101	(67 ± 4)
														Average	48 ± 1				48 ± 1
										2WA									
529a*	U17	70·9 ± 1·8	0·01	0·26/0·01	1000	50	n.d.	n.d.	n.d.	1130 ± 100	0 ± 0	2 ± 3	3 ± 0	1135 ± 100	62 ± 6	1 ± 1	1 ± 0	1132 ± 100	63 ± 6
529b*		70·1 ± 1·5	0·04	0·20/0·13	1190	50	n.d.	n.d.	n.d.	1130 ± 100	0 ± 0	10 ± 2	2 ± 0	1145 ± 100	61 ± 6	4 ± 2	1 ± 0	1136 ± 100	62 ± 6
541a*	S18	74·9 ± 1·9	0·01	0·05/0·01	1250	50	2·06	14	1·68	1195 ± 60	0 ± 0	3 ± 2	0 ± 1	1198 ± 60	63 ± 4	1 ± 1	0 ± 0	1196 ± 60	63 ± 4
541b*		76·5 ± 3·7	0·09	0·05/0·01	1150	50	2·06	14	1·68	1195 ± 60	0 ± 0	23 ± 4	0 ± 2	1218 ± 60	63 ± 4	10 ± 2	0 ± 0	1205 ± 60	64 ± 4
														Average	63 ± 2				63 ± 2

Table 1 (*Continued*)

Sample no.	Square	D_E (Gy)	U (EN) (ppm)	U (DE) (ppm)	TT (µm)	S1/S2 (µm)	Sediment U (ppm)	Th (ppm)	K (%)	γ-Ḋ (µGy/a)	β-Ḋ (µGy/a)	Early U-uptake int.Ḋ (µGy/a)	DE-Ḋ (µGy/a)	Total Ḋ (µGy/a)	Age (ka)	Linear U-uptake int.Ḋ (µGy/a)	DE-Ḋ (µGy/a)	Total Ḋ (µGy/a)	Age (ka)
										3BS 1									
535A	U17	78·1 ± 1·4	0·01	0·01	1200	50	2·44	12	2·01	1250 ± 100	233 ± 24	2 ± 3	0 ± 0	1485 ± 103	53 ± 4	1 ± 1	0 ± 0	1484 ± 103	53 ± 4
535B		90·0 ± 2·5	0·01	0·16	1200	50	2·44	12	2·01	1250 ± 100	233 ± 24	2 ± 4	2 ± 2	1487 ± 103	61 ± 5	1 ± 1	1 ± 0	1485 ± 103	61 ± 5
535C		90·0 ± 2·5	0·01	0·16	1200	50	2·44	12	2·01	1250 ± 100	233 ± 24	2 ± 4	2 ± 2	1487 ± 103	61 ± 5	1 ± 1	1 ± 0	1485 ± 103	61 ± 5
535D		85·9 ± 2·6	0·01	0·01	1250	50	2·44	12	2·01	1250 ± 100	223 ± 22	2 ± 3	0 ± 0	1475 ± 103	58 ± 4	1 ± 1	0 ± 0	1474 ± 102	58 ± 4
														Average	58 ± 2				58 ± 2
										3BS 2									
608A†	U15	92·8 ± 1·5	0·01	0·08	800	50	2·60	19	2·80	1200 ± 100	240 ± 53	2 ± 3	1 ± 0	1443 ± 113	64 ± 5	1 ± 1	0 ± 1	1441 ± 113	64 ± 5
608B†		104 ± 5	0·01	0·01	1000	50	2·60	19	2·80	1200 ± 100	195 ± 41	3 ± 2	0 ± 0	1398 ± 108	74 ± 7	1 ± 1	0 ± 0	1396 ± 108	74 ± 7
608C†		93·9 ± 2·2	0·21	0·01	1000	50	2·60	19	2·80	1200 ± 100	195 ± 41	51 ± 7	0 ± 0	1448 ± 108	65 ± 5	22 ± 3	0 ± 0	1418 ± 108	66 ± 5
														Average	66 ± 3				67 ± 4
										3BS 3									
607A	U16	119 ± 3	0·01	0·10	900	50	2·60	19	2·80	1230 ± 100	426 ± 46	3 ± 2	1 ± 0	1660 ± 110	72 ± 5	1 ± 1	1 ± 0	1658 ± 110	72 ± 5
607B		126 ± 5	0·01	0·01	900	50	2·60	19	2·80	1230 ± 100	426 ± 46	3 ± 2	0 ± 0	1659 ± 110	76 ± 6	1 ± 1	1 ± 0	1657 ± 110	76 ± 6
														Average	74 ± 4				74 ± 4
										3WA									
536A	U21	108 ± 3	0·01	0·22	1050	50	2·05	12	1·57	1340 ± 100	221 ± 23	3 ± 2	2 ± 1	1566 ± 103	69 ± 5	1 ± 1	1 ± 0	1563 ± 103	69 ± 5
536B		70·4 ± 2·3	0·01	0·14	1250	50	2·05	12	1·57	1340 ± 100	183 ± 17	2 ± 3	1 ± 0	1526 ± 102	(46 ± 3)	1 ± 1	1 ± 1	1525 ± 101	(46 ± 3)
536C		110 ± 3	0·01	0·22	1200	50	2·05	12	1·57	1340 ± 100	192 ± 19	3 ± 2	2 ± 0	1537 ± 102	71 ± 5	1 ± 1	1 ± 0	1534 ± 102	71 ± 5
609A	U21	104 ± 4	0·01	0·10	1150	50	2·20	14	2·20	1340 ± 100	261 ± 26	3 ± 2	1 ± 0	1605 ± 103	65 ± 5	1 ± 1	0 ± 0	1602 ± 103	65 ± 5
609B		91·7 ± 6·3	0·01	0·10	970	50	2·20	14	2·20	1340 ± 100	312 ± 34	2 ± 3	1 ± 0	1655 ± 106	55 ± 5	1 ± 1	0 ± 2	1653 ± 106	55 ± 5
609C		107 ± 5	0·01	0·14	1050	50	2·20	14	2·20	1340 ± 100	288 ± 31	3 ± 2	2 ± 2	1633 ± 105	65 ± 5	1 ± 1	1 ± 0	1630 ± 105	65 ± 5
														Average	66 ± 2				67 ± 2
										1RGBS									
601A	F16	136 ± 4	0·01	0·01	1000	50	2·50	17	3·30	1565 ± 200	425 ± 45	3 ± 2	0 ± 0	1993 ± 205	68 ± 7	1 ± 1	0 ± 0	1991 ± 205	68 ± 7
601B		174 ± 6	0·01	0·14	750	50	2·50	17	3·30	1565 ± 200	553 ± 62	3 ± 2	2 ± 0	2123 ± 209	82 ± 8	1 ± 1	1 ± 0	2120 ± 209	82 ± 9
601C		170 ± 3	0·01	0·14	750	50	2·50	17	3·30	1565 ± 200	553 ± 62	3 ± 2	2 ± 0	2123 ± 209	80 ± 8	1 ± 1	1 ± 0	2120 ± 209	80 ± 8
														Average	76 ± 4				75 ± 5
										4BS									
534a	F16	133 ± 4	0·01	0·16	750	50	2·44	14	1·52	1230 ± 62	312 ± 34	3 ± 2	2 ± 2	1547 ± 71	86 ± 5	1 ± 1	1 ± 0	1544 ± 71	86 ± 5
534b		131 ± 4	0·01	0·20	750	50	2·44	14	1·52	1230 ± 62	312 ± 34	3 ± 2	3 ± 0	1548 ± 71	85 ± 5	1 ± 1	1 ± 0	1544 ± 71	85 ± 5
647A	Q15	116 ± 6	0·05	0·10	800	50	1·59	8·0	1·42	1200 ± 61	240 ± 27	13 ± 4	1 ± 1	1454 ± 67	79 ± 5	6 ± 1	1 ± 0	1447 ± 67	80 ± 5
647B		106 ± 4	0·10	0·10	700	50	1·59	8·0	1·42	1200 ± 61	267 ± 30	25 ± 5	2 ± 2	1494 ± 68	71 ± 4	11 ± 2	1 ± 0	1479 ± 68	72 ± 4
538a	R19	120 ± 3	0·01	0·01	950	50	1·67	7·2	1·21	1280 ± 64	182 ± 20	3 ± 2	0 ± 0	1465 ± 67	81 ± 4	1 ± 1	0 ± 0	1463 ± 67	82 ± 4
538b*		117 ± 3	0·05	0·05/0·05	1250	50	1·67	7·2	1·21	1280 ± 64	0 ± 0	15 ± 3	1 ± 1	1297 ± 64	91 ± 5	6 ± 2	0 ± 0	1286 ± 64	91 ± 5
538c*		117 ± 4	0·06	0·07/0·05	1200	50	1·67	7·2	1·21	1280 ± 64	0 ± 0	17 ± 4	1 ± 0	1299 ± 64	90 ± 5	7 ± 2	0 ± 0	1287 ± 64	91 ± 6
														Average	82 ± 2				82 ± 2

Table 1 (*Continued*)

Sample no.	Square	D_E (Gy)	U (EN) (ppm)	U (DE) (ppm)	TT (µm)	S1/S2 (µm)	Sediment U (ppm)	Th (ppm)	K (%)	γ-$\dot{D}$ (µGy/a)	β-$\dot{D}$ (µGy/a)	Early U-uptake int.$\dot{D}$ (µGy/a)	DE-$\dot{D}$ (µGy/a)	Total $\dot{D}$ (µGy/a)	Age (ka)	Linear U-uptake int.$\dot{D}$ (µGy/a)	DE-$\dot{D}$ (µGy/a)	Total $\dot{D}$ (µGy/a)	Age (ka)
										4WA									
602a	U16	141 ± 2	0·01	0·14	1100	50	2·00	12	1·60	1050 ± 51	212 ± 22	3 ± 3	2 ± 0	1267 ± 56	111 ± 6	1 ± 2	1 ± 0	1264 ± 56	111 ± 6
602b		162 ± 9	0·01	0·01	1100	50	2·00	12	1·60	1050 ± 51	212 ± 22	3 ± 4	0 ± 0	1265 ± 56	128 ± 9	1 ± 2	0 ± 0	1263 ± 56	128 ± 9
602c		156 ± 8	0·11	0·03	1100	50	2·00	12	1·60	1050 ± 51	212 ± 22	36 ± 6	0 ± 1	1297 ± 56	120 ± 8	15 ± 3	0 ± 0	1277 ± 56	122 ± 9
														Average	118 ± 4				118 ± 4
										4WA 6									
603A	T15	210 ± 28	0·12	0·01	700	50	2·10	13	2·40	1100 ± 54	435 ± 49	39 ± 7	0 ± 0	1575 ± 74	133 ± 19	17 ± 3	0 ± 0	1551 ± 73	135 ± 20
603B		241 ± 10	0·01	0·08	800	50	2·10	13	2·40	1100 ± 54	390 ± 43	4 ± 3	1 ± 1	1460 ± 69	165 ± 10	1 ± 3	1 ± 0	1457 ± 69	165 ± 10
603C		149 ± 7	0·01	0·08	700	50	2·10	13	2·40	1100 ± 54	435 ± 49	3 ± 3	1 ± 1	1539 ± 73	97 ± 6	1 ± 1	1 ± 0	1537 ± 73	97 ± 6
														Average	116 ± 5				116 ± 5
										4WA 7									
604A	Q15	251 ± 8	0·01	0·06	800	50	1·60	12	1·70	1100 ± 56	290 ± 32	4 ± 3	1 ± 0	1395 ± 65	180 ± 10	2 ± 1	0 ± 1	1392 ± 65	180 ± 10
604B		234 ± 9	0·01	0·06	1000	50	1·60	12	1·70	1100 ± 56	236 ± 25	4 ± 3	1 ± 0	1341 ± 61	174 ± 10	2 ± 1	0 ± 0	1338 ± 61	175 ± 10
604C		233 ± 4	0·05	0·01	950	50	1·60	12	1·70	1100 ± 56	248 ± 27	18 ± 5	0 ± 0	1366 ± 62	171 ± 8	8 ± 1	0 ± 0	1356 ± 62	172 ± 8
														Average	174 ± 5				175 ± 5
										5BS 2									
605a	N16	274 ± 13	0·05	0·31	1000	50	2·10	13	2·60	1230 ± 61	336 ± 36	18 ± 5	5 ± 1	1589 ± 71	173 ± 11	8 ± 1	2 ± 0	1576 ± 71	175 ± 11
605b		263 ± 13	0·35	0·37	1100	50	2·10	13	2·60	1230 ± 61	304 ± 32	125 ± 18	5 ± 0	1664 ± 71	159 ± 10	54 ± 7	2 ± 0	1590 ± 69	166 ± 11
605c		267 ± 10	0·07	0·40	1000	50	2·10	13	2·60	1230 ± 61	336 ± 36	25 ± 6	6 ± 0	1597 ± 71	168 ± 10	11 ± 2	3 ± 1	1580 ± 71	170 ± 10
														Average	166 ± 6				170 ± 6
										5BS 5									
539a	S15	195 ± 10	0·01	0·01	900	50	0·95	5·0	0·92	1220 ± 60	138 ± 16	3 ± 4	0 ± 0	1361 ± 62	143 ± 10	1 ± 2	0 ± 0	1359 ± 62	143 ± 10
539b		218 ± 16	0·01	0·01	900	50	0·95	5·0	0·92	1220 ± 60	138 ± 16	4 ± 3	0 ± 0	1362 ± 62	160 ± 14	1 ± 3	0 ± 0	1359 ± 62	160 ± 14
539c		200 ± 9	0·01	0·03	800	50	0·95	5·0	0·92	1220 ± 60	153 ± 17	3 ± 4	1 ± 1	1377 ± 63	145 ± 9	1 ± 2	0 ± 0	1374 ± 63	145 ± 9
														Average	147 ± 6				147 ± 6
										5WA 1									
754a*	T14	267 ± 29	0·09	0·07/0·14	950	50	1·37	7·2	1·60	1285 ± 64	0 ± 0	34 ± 8	1 ± 0	1322 ± 64	202 ± 24	15 ± 2	1 ± 1	1302 ± 64	205 ± 24
754b*		272 ± 31	0·20	0·10/0·14	550	50	1·37	7·2	1·60	1285 ± 64	0 ± 0	73 ± 12	2 ± 1	1363 ± 65	200 ± 25	31 ± 5	1 ± 0	1318 ± 64	207 ± 26
754c		264 ± 10	0·20	0·24	850	50	1·37	7·2	1·60	1285 ± 64	240 ± 29	71 ± 11	4 ± 0	1600 ± 71	165 ± 10	30 ± 5	2 ± 0	1557 ± 70	170 ± 10
														Average	174 ± 9				179 ± 9
										5WA 2									
753	S14	350 ± 7	0·09	0·48	550	25	0·77	4·1	1·01	1285 ± 64	210 ± 21	34 ± 6	12 ± 1	1541 ± 68	227 ± 11	15 ± 2	5 ± 1	1515 ± 67	231 ± 11

For details on ESR age calculation, U-uptake modes see Grün (1989) and text. EN=enamel; DE=dentine; TT=total enamel thickness; S1/S2=surface layer removed from each side of the enamel samples. n.d.: not determined. Neutron activation uncertainties: U: 0·01 ppm, Th: 0·1 ppm, K: 0·05%.

*Enamel was separated from an interior layer of the tooth. External beta dose rate originates from two dentine layers.

†The enamel was coated with a thin layer of cementum. The external beta dose rate was corrected accordingly.

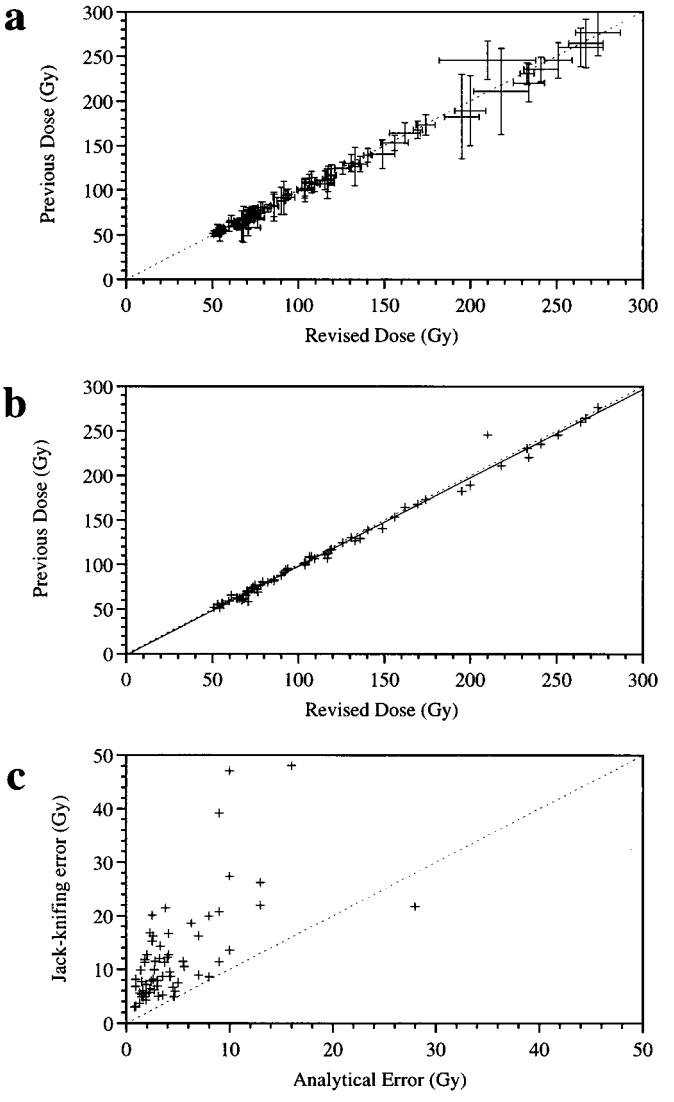

Figure 2. Comparison of revised dose [(a) and (b)] and error calculations (c). The new dose estimates were obtained with simplex fitting optimization using weights inverse proportional to the squared intensity and error calculation derived from analytical expressions (after Brumby, 1992; for more details see Grün & Brumby, 1994; Grün, 1998*a*). The older dose estimations were also based on simplex optimization procedures using equal weights and error calculation was derived from jack-knifing (Grün & Macdonald, 1988). In (b), the error bars are removed for clarity. A linear regression of the data (dotted line in b) is nearly indistinguishable from the 1:1 line (solid one). The jack-knifing error of all but one sample is significantly larger than the error derived from analytical expression (c).

measurements have to be carried out close to the samples. For 1RGBS, no gamma measurement was carried out. This unit is part of 4BS and a similar gamma dose rate could be expected. However, the analytical values for the sediment linked to sample 601 imply a significantly higher dose rate. Thus, in this study the gamma dose rate was

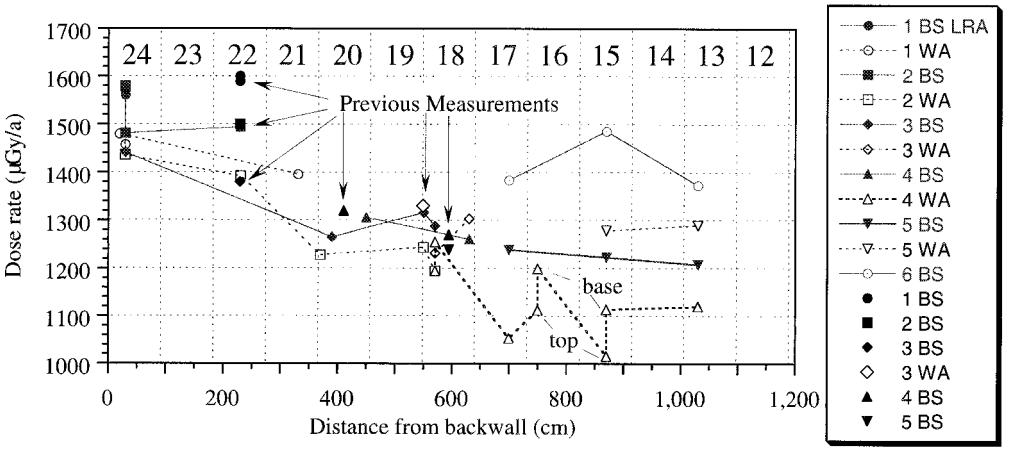

Figure 3. Results of the 1994 gamma survey. The distribution of the gamma dose rates is complex. There is a general trend of decreasing gamma dose rate from the back-wall of the cave towards the mouth. 4WA shows the largest variation within the layer by having significantly higher gamma dose rate values at the base (see strips 16 and 17). The new measurements were carried out in strips S and T [for positions of the strips (12 to 24) see Figure 1]. There is a very good agreement between the 1994 and 1988 measurements although different gamma spectrometers were used and several of the older measurements were carried out in strips N and O.

averaged from the analytical values of the sediment sample and the gamma dose rate derived from layer 4BS. One should note, that there are also larger discrepancies between the analysis of the sediment and measured gamma dose rates for layers 5BS and 5WA and this may be the cause of some of the large scattering of age results observed from the samples from these layers.

Beta dose rates

Beta dose rates were calculated using the Monte Carlo attenuation curves presented by Brennan *et al.* (1997). This leads to much smaller external beta dose rates. Figure 4(b) shows the comparison of the earlier and revised beta dose rates. The data were fitted with a straight line (forced through zero) which shows that the older beta dose rates are on average 60% higher than those based on Monte Carlo attenuation factors.

Dose rate conversion factors

The new dose rate conversion factors of Adamiec & Aitken (1998) show the largest change (-4%) in the beta dose rate from K; the overall effect of the re-calculated dose rates on the total dose rate is negligible (<1%).

Total dose rates and age estimations

Figure 4(c) shows the comparison of total dose rates. The differences between the older and revised total dose rates translate directly into age differences, because the average dose estimations (Figure 2) have not changed. The changes in dose rates range between zero and about -30% (with an average of -15%).

Comparisons with other chronologies

Figure 5 shows the revised chronology for Border Cave. Figure 5 also includes samples 753 and 754 from 5WA which were analysed after the original study of Grün *et al.* (1990). Samples from Border Cave were also analysed by a variety of other dating techniques, particularly radiocarbon (Beaumont, 1980) and amino acid racemization (Miller *et al.*, 1999), see Table 2. The

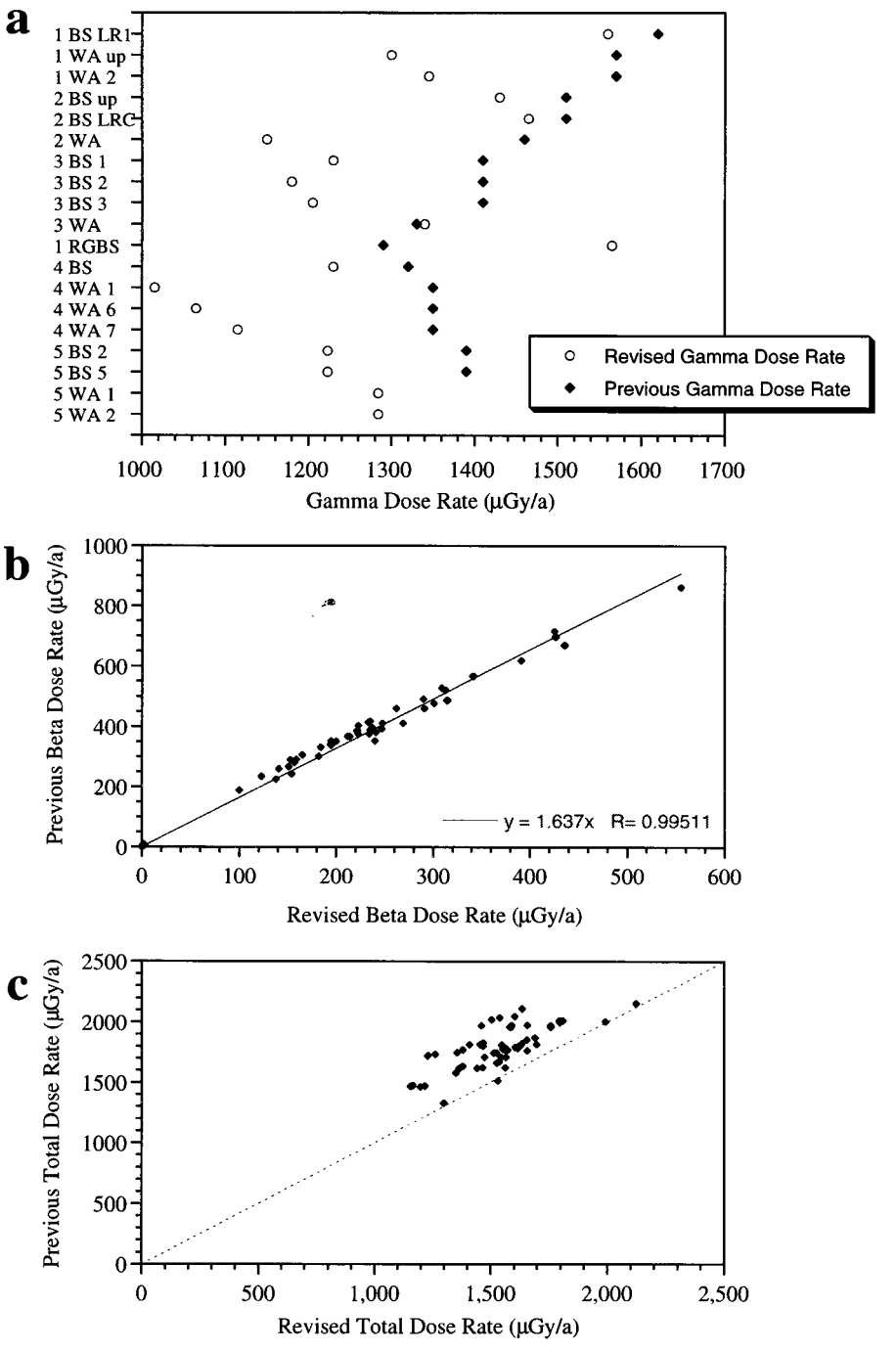

Figure 4. (a) The revised gamma dose rates are throughout lower than in the previous study, because most of the 1988 measurements were carried out closer to the back-wall (see Figure 3). The beta dose rates have a very high correlation but the older calculations yielded 60% higher dose rate values (b). The total dose rates are on average 15% lower than in the previous study, resulting in a corresponding age increase (c).

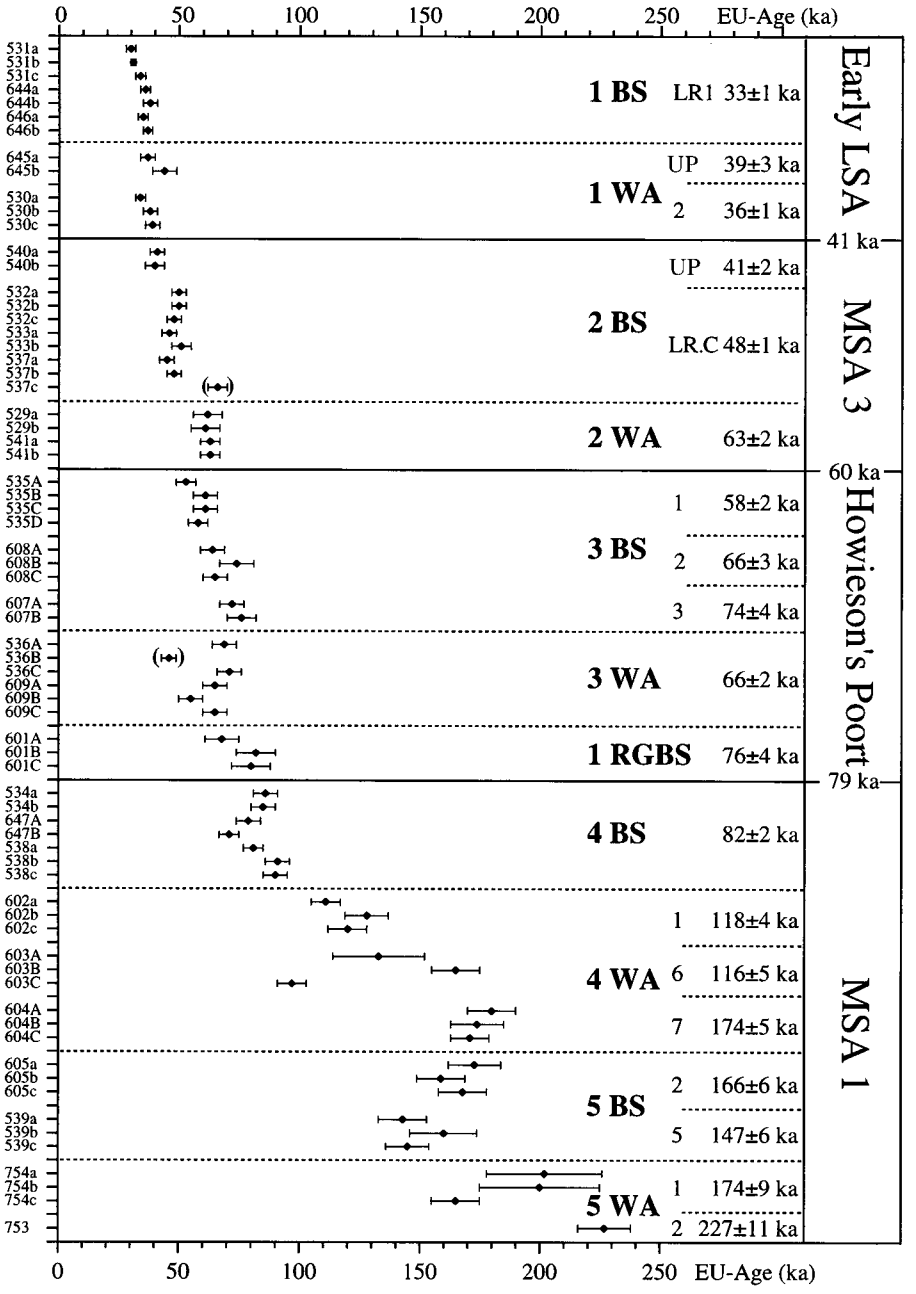

Figure 5. Revised ESR chronology for Border Cave. Lower-case letters following the sample number denote sub-samples of a single tooth, capital letters separate enamel fragments. The two bracketed results were not used for the calculation of the average ages of the units.

Table 2 Comparison of ESR data with independent age estimates of Beaumont (1980) and Miller *et al.* (1999)

Unit	^{14}C (Beaumont)	^{14}C (Miller)	AAR (Miller)	Revised ESR
1BS. LR	33–38	38 ± 1		33 ± 1 ka
1WA	33–45	38–40		35–42 ka
2BS. UP	43–>49	>49	47 ± 5	41 ± 2 ka
2BS LRC			56 ± 6	48 ± 1 ka
2WA			69 ± 7	63 ± 2 ka
4BS/4 WA1			>100	80–122 ka

AAR=amino acid racemization.

ESR results are compatible with most of the radiocarbon results reported by Beaumont (1980). In comparison with the data of Miller *et al.* (1999), the revised ESR chronology agrees within error but seems systematically on the young side. One has to keep in mind, however, that first, many horizons are presented by a single tooth for ESR, and second, for the radiocarbon chronology usually only the oldest age estimates were used for assessing the age of a horizon. While the latter procedure is based on the assumption that any younger radiocarbon results are caused by recent CO_2 exchange, age spread could also be attributable to reworking processes. Reworking would, of course, also apply to some of the ESR results (which may have caused, e.g., the age spread of the tooth enamel fragments of sample 603 in 4WA6).

Discussion of new and revised ESR data

The major points of contention that arose from the 1990 ESR chronology are:

(1) the ESR results were significantly younger than the radiocarbon data on the same layers (Beaumont, 1980);
(2) the ESR results were significantly younger than the amino acid chronology (Miller & Beaumont, 1989);
(3) the age for the Howieson's Poort industry was too young and its duration too long (e.g., Beaumont *et al.*, 1978).

The comparison of the revised ESR dataset with independent chronologies now shows good agreement. The revised ESR readings now provide a chronological framework for Border Cave that is in broad agreement with results obtained by way of radiocarbon, U-series, amino acid epimerization (see Beaumont *et al.*, 1978, 1992; Beaumont, 1980; Miller & Beaumont, 1989; Miller *et al.*, 1999) and unpublished TL assays on burnt opalines by Huxtable & Valladas (personal communications to P.B.B.).

Chronology for the human remains

The ESR dates are not relevant for the Iron Age BC4. BC6 to BC8 were recovered by trowelling away about 100 m^3 of disturbed deposit formed since 1934 (Beaumont, 1994). These specimens consist of a humerus (BC6), a proximal ulna (BC7) and two metatarsals (BC8a & b) and have been described by Morris (1992), Pearson & Grine (1996) and Pfeiffer & Zehr (1996). However, it is difficult to establish the provenance for BC6 to BC8. Thus, we have refrained from speculation about their antiquity. The revised ESR dates have the following implications for the ages of the other human remains at the site.

BC1 and BC2

BC1 and BC2, an incomplete cranial vault and a partial mandible respectively, are both unprovenanced specimens from Horton's Pit, of which the former has been linked to the "soft dark earth" of the 4BS on the basis of comparable soil adhesions in the small interstices of the skull (Cooke *et al.*, 1945). However, slumped sediment removal in 1987 led to the discovery that the 4WA–5WA sequence had been removed to varying extents towards the centre of Horton's Pit (Figure 1), thereby contravening a 1942 claim that the 4WA formed its base (Beaumont, 1980) and implying that BC1 may have come from the very similar 5BS, as is suggested by its very low nitrogen readings (Beaumont, 1994; Sillen & Morris, 1996). The strata 4WA.C to 5WA now have ESR ages of from about 145 to 230 ka and concordant unpublished TL readings by J. Huxtable (personal communication) of about 165 to 180 ka for 4WA.C and about 180 ka for 5WA. Proxy palaeoenvironmental evidence (Avery, 1992) implies that these layers would be best placed in oxygen isotope stage 7. However, the exact provenance of BC1 and BC2 (whether derived from 4BS or 5BS) can only be established by precise, direct dating analysis, possibly combined Th/U–Pa/U dating (see Cheng & Edwards, 1998; Simpson & Grün, 1998).

BC3

This infant skeleton from the 1941 excavation came from a $\geq 0{\cdot}24$ m deep grave straddling squares F12 and G12 that was entirely cut into the 4BS, with its lip reported as undoubtedly lying below an ash horizon at the very base of the Howieson's Poort sequence (Cooke *et al.*, 1945). An examination of the lithic samples from squares F12 and G12 revealed that the spits overlying the grave contain only artefacts (including segments) of Howieson's Poort ascription, with there being no trace of the expected 1BS and 4BS-derived admixture if it had been intrusive (Beaumont, 1994). The sole object in definite association with BC3 was a perforated *Conus* seashell (Cooke *et al.*, 1945), later identified as *C. bairstowi* (Beaumont *et al.*, 1992), a species now endemic to a stretch of eastern Cape coast about 760–980 km to the south west (Richards, 1981; Kilburn & Rippey, 1982). This finding implies, in the absence of evidence of such distant trade in stone age times, that the shell was collected from a Tongaland beach about 80 km away during a stadial when Indian Ocean temperatures were much cooler than now, resulting in that species having a distribution about 5–6° closer to the equator (Beaumont *et al.*, 1992). Amino acid analysis of the BC3 pendant, and of an identical and probably *in situ* specimen that was recovered from the IRGBS.UP in square C11 during fieldwork in 1987 (Beaumont, 1994), produced almost identical aIle/Ile ratios (B. Johnson, personal communication). Subsequent AMS dating of a portion of the former produced, given the material, a good minimum reading $33{,}570 \pm 120$ BP (AA-14033). If so, then BC4 was buried at that time of the deposition of IRGBS and its ESR age is about 76 ka (Figure 5).

BC5

This largely complete lower jaw (BC5) was recovered by C. Powell in 1974 from the northwest edge of square T20, while she and one of us (PBB) were collecting sediment samples, at the request of K. W. Butzer, from the south face of Excavation 3A (Figure 1). It was located some $0{\cdot}25$ m below the intact surface of the 3WA and abutted on a previously mapped and photographed depression, with rather poorly defined edges and a depth of up to $0{\cdot}15$ m, at the very base of that stratum. The excavation of square T20 about 6 months later, and of T21, U20 and U21 by G. Miller in 1987, permitted the full extent of this $1{\cdot}8$ m wide sub-circular feature to be traced

(Figure 1), but, unexpectedly, no further human remains were found in it.

Detailed analysis of the artefact types, their numbers, orientations and dips, proportion of opaline artefacts, contents of macrofaunal and charcoal fragments, as well as ^{14}C and U-series age results show that square T20 displays the same distinctive patterns as nearby undisturbed layers (Beaumont, unpublished data). This seems to rule out that BC5 could have been buried from an Iron Age layer (as implied by the study of nitrogen contents and infra-red splitting factors by Sillen & Morris, 1996). If BC5 was indeed buried at the time when layer 3WA was deposited, its age is about 66 ka. Direct ESR measurements on an enamel fragment (Grün, 1995; Robertson & Grün, 2000) from BC5 could lay the question of its provenance conclusively to rest.

Implications

Given the age of 5BS and the consequent early *H. sapiens* affinities of BC1 and BC2 (de Villiers, 1973, 1976) and also perhaps BC6 (Pearson & Grine, 1996), this would tentatively support the inference that humans of fully modern cranial form had already occupied some subtropical portions of the subcontinent by before 130 ka. The persistence of populations with some archaic features long after then in the southern Cape (Smith *et al.*, 1989) could then be seen as support for the postulate that the formative phases of modern human evolution were confined to the savannas, *sensu lato* (Beaumont *et al.*, 1978), and perhaps even to a southern portion of it (e.g., Gibbons, 1997). In this case present evidence bearing on the genesis of our kind would be sparse, and it bears reiterating (Beaumont, 1980) that a firmer focus on fieldwork in appropriate regions is called for (e.g., Yellen *et al.*, 1995), as also further efforts to more firmly date the few known early humans from that biome, particularly BC1 and Omo 1.

Timing and duration of the Middle and Later Stone Age industries

The new ESR chronology is more compatible with ^{14}C ages for the Early LSA occupation pulse (e.g., Wintle, 1996), that could be related to a palaeoclimatic amelioration coeval with Dansgaard-Oeschger event 12 at about 42 to 44 ka (Bischoff *et al.*, 1994; Blunier *et al.*, 1998). In a recent compilation of amino acid racemization data from Boomplaas, Apollo 11 and Border Cave, Miller *et al.* (1999) concluded that the age of the Howieson's Poort industry was bracketed by limiting dates of 56 and 80 ka and was most likely centred on 66 ± 5 ka. The revised dataset confirms this estimate with a time span of between 60 and 79 ka (these boundaries also consider the ages of the over- and underlying layers). However, the duration of the Howieson's Poort seems somewhat longer (around 20 ka) than usually assumed (around 10 ka: Beaumont *et al.*, 1978; Deacon, 1989). Concordant ESR and TL readings for 4WA.C and 5WA now show with reasonable certainty that the lowermost MSA levels (without handaxes) at Border Cave extend beyond about 195 ka (Butzer *et al.*, 1978) to perhaps basal oxygen isotope stage 7 in the as yet undated 6BS (for duration and boundaries of oxygen isotope stages (see Martinson *et al.*, 1987; Shackleton *et al.*, 1990).

Palaeoclimatic information

The new ESR readings also corroborate that a higher than present temperature and a $\geq 3^{\circ}$ southward shift of miombo woodland previously inferred for 4WA.A&B microfaunal samples (Avery, 1992) does indeed equate (Beaumont *et al.*, 1992) with oxygen isotope stage 5e at about 129 to 119 ka ago (Adkins *et al.*, 1997).

The chronometric results as a whole identify four hiatuses, at the 4WA.A.B–C, 4BS–4WA and 2BS.LR.C–2WA interfaces, and also near the surface of IBS.LR.A (Beaumont *et al.*, 1978), in an otherwise

seemingly continuous sequence that is divisible into two broad sediment formation settings. The earlier, from 6BS–4WA, represents two successive full interglacials (oxygen isotope stages 7 and 5e), formed when temperatures were similar to now and rainfall was about 125–200% higher, with an outside cover dominated by miombo woodland that sustained high occupation densities of about 3100–8600 lithics per m^3 (Avery, 1992; Beaumont *et al.*, 1992). The later, from 4BS–1BS.LR.A, built up under the less congenial conditions of late oxygen isotope stage 5 to 2 when temperatures were cooler than now and rainfall was up to 65% lower, with an outside cover having a higher grassland component that sustained lower occupation densities of about 200–2300 lithics per m^3 (Avery, 1992; Beaumont *et al.*, 1992).

Conclusions

We draw the following conclusions from this study:

(1) The revised ESR readings now provide a chronological framework for Border Cave that is in broad agreement with results obtained by radiocarbon, U-series, amino acid epimerization and unpublished TL assays on burnt opalines by Huxtable and Valladas.

(2) If BC3 and BC5 are *in situ* their ESR ages are about 76 and 66 ka, respectively.

(3) New sedimentological studies imply that BC1 may have come from 5BS. Thus, modern humans could have occurred in southern Africa as early as 170 ka ago. On the other hand, if BC1 and 2 were derived from 4BS, their ages would be around 82 ka.

(4) The results of this study and the controversy about the origin of the human remains at Border Cave, particularly of BC5 (Sillen & Morris, 1996), reiterate the urgent necessity to further develop and apply direct dating to the human remains.

(5) The ESR results confirm the great antiquity (between 60 and 79 ka) of the Howieson's Poort-bearing strata. However, the duration of the Howieson's Poort seems somewhat longer (around 20 ka) than usually assumed (around 10 ka: Beaumont *et al.*, 1978; Deacon, 1989). The MSA/LSA transition can be placed at about 41 ka and the lowermost MSA levels extend well beyond 200 ka, perhaps to the beginning of the penultimate interglaciation.

Acknowledgements

P.B.B. wishes to thank the Anglo American Chairman's Fund for supporting the 1987 excavations at Border Cave, Lewis Binford for his support of the project, Lawrence Todd and Glen Miller for 60 days of dedicated help, Gifford Miller and Barbara Johnson for their work on the BC3 *Conus*. Andrew Sillen for the SF and N assays and Joan Huxtable for providing her preliminary TL results. We thank J. Chappell, RSES, for comments. We thank the Centre for Archaeological Research, ANU, for support.

References

Adamiec, G. & Aitken, M. J. (1998). Dose-rate conversion factors: update. *Ancient TL* **16,** 37–50.

Adkins, J. E., Boyle, E. A., Keigwin, L. & Cortijo, E. (1997). Variability of the North Atlantic thermohaline circulation during the last interglacial period. *Nature* **390,** 154–156.

Aitken, M. J., Clark, P. A., Gaffney, C. F. & Lovborg, L. (1985). Beta and gamma gradients. *Nuclear Tracks and Rad. Meas.* **10,** 647–653.

Avery, D. M. (1992). The environment of early modern humans at Border Cave, South Africa: micromammalian evidence. *Palaeogr. Palaeoclimatol. Palaeoecol.* **91,** 71–87.

Beaumont, P. B. (1980). On the age of Border Cave hominids 1–5. *Palaeontol. Afr.* **23,** 21–33.

Beaumont, P. B. (1994). Report to the KwaZulu Monuments Council on excavations at Border Cave near Ingwavuma in July–August 1987 and on the

results of related investigations up until December 1993. Kimberley: McGregor Museum.

Beaumont, P. B., de Villiers, H. & Vogel, J. C. (1978). Modern man in sub-Saharan Africa prior to 49 000 years B.P.: a review and evaluation with particular reference to Border Cave. *S. Afr. J. Sci.* **74,** 409–419.

Beaumont, P. B., Miller, G. H. & Vogel, J. C. (1992). Contemplating old clues to the impact of future greenhouse climates in South Africa. *S. Afr. J. Sci.* **88,** 490–498.

Bischoff, J. L., Ludwig, K., Garcia, J. F., Carbonell, E., Vaquero, M., Stafford, T. W. Jr & Jull, A. J. T. (1994). Dating of the basal Aurignacian sandwich at Abric Romaní (Catalunya, Spain) by radiocarbon and U-series. *J. Archaeol. Sci.* **21,** 541–551.

Blunier, T., Chappelaz, J., Schwander, J., Dallenbach, A., Stauffer, B., Stocker, T. F., Raymond, D., Jouzel, J., Clausen, H. B., Hammer, C. V. & Johnsen, S. J. (1998). Asynchrony of Antarctic and Greenland climate change during the last glacial period. *Nature* **394,** 739–743.

Brennan, B. J., Rink, W. J., McGuirl, E. L., Schwarcz, H. P. & Prestwich, W. V. (1997). Beta doses in tooth enamel by "One Group" theory and the Rosy ESR dating software. *Rad. Meas.* **27,** 307–314.

Brennan, B. J., Prestwich, W. V., Rink, W. J., Marsh, R. E. & Schwarcz, H. P. (2000). Alpha and beta dose gradients in tooth enamel. *Rad. Meas.* **32,** 759–765.

Brumby, S. (1992). Regression analysis of ESR/TL dose–response data. *Nuclear Tracks and Rad. Meas.* **20,** 595–599.

Butzer, K. W., Beaumont, P. B. & Vogel, J. C. (1978). Lithostratigraphy of Border Cave, KwaZulu, South Africa: a Middle Stone Age sequence beginning c. 195,000 B.P. *J. Archaeol. Sci.* **5,** 317–341.

Cheng, H. & Edwards, R. L. (1998). U/Th and U/Pa dating of Nanjing Man and Peking Man. Abstracts of ICOG-9. *Chinese Science Bulletin* **43**(Suppl.)26.

Cooke, H. B. S., Malan, B. D. & Wells, L. H. (1945). Fossil man in the Lebombo Mountains, South Africa: the "Border Cave", Ingwavuma district, Zululand. *Man* **45,** 6–13.

De Villiers, H. (1973). Human skeletal remains from Border Cave, Ingwavuma district, KwaZulu, South Africa. *Ann. Transv. Mus.* **28,** 229–256.

De Villiers, H. (1976). A second adult human mandible from Border Cave, Ingwavuma district, KwaZulu, South Africa. *S. Afr. J. Sci.* **72,** 121–125.

Deacon, H. J. (1989). Late Pleistocene palaeoecology and archaeology in the Southern Cape, South Africa. In (P. Mellars & C. B. Stringer, Eds) *The Human Revolution: Behavioural and biological perspectives on the origins of modern humans, Vol. I*, pp. 547–564. Edinburgh: Edinburgh University Press.

Gibbons, A. (1997). Y chromosome shows that Adam was an African. *Science* **278,** 804–805.

Grün, R. (1986). Beta dose attenuation in thin layers. *Ancient TL* **4,** 1–8.

Grün, R. (1989). Electron spin resonance (ESR) dating. *Quatern. Int.* **1,** 65–109.

Grün, R. (1995). Semi non-destructive, single aliquot ESR dating. *Ancient TL* **13,** 3–7.

Grün, R. (1997). Electron spin resonance dating. In (R. E. Taylor & M. J. Aitken, Eds) *Chronometric and Allied Dating in Archaeology*, pp. 217–261. New York: Plenum.

Grün, R. (1998*a*). Reproducibility measurements for ESR signal intensity and dose determination: high precision but doubtful accuracy. *Rad. Meas.* **29,** 177–193.

Grün, R. (1998*b*). Dose determination on fossil tooth enamel using spectrum deconvolution with Gaussian and Lorentzian peak shapes. *Ancient TL* **16,** 51–55.

Grün, R. (2000*a*). Methods of dose determinations using ESR spectra of tooth enamel. *Rad. Meas.* **32,** 767–772.

Grün, R. (2000*b*). Electron spin resonance dating. In (L. Ellis, Ed.) *Archaeological Method and Theory: An Encyclopedia*, pp. 174–178. New York: Garland.

Grün, R. (2000*c*). Electron spin resonance dating. In (E. Ciliberto & G. Spoto, Eds) *Modern Analytical Methods in Art and Archaeology*. Chemical Analyses Series 155, pp. 641–679. New York: Wiley.

Grün, R. (2000*d*). Dating beyond the radiocarbon barrier using U-series isotopes and trapped charges. In (D. C. Creagh & D. A. Bradley, Eds) *Radiation in Art and Archeometry*, pp. 472–493. Amsterdam: Elsevier.

Grün, R. (2001*a*). Trapped charge dating (ESR, TL, OSL). In (M. Pollard & D. Brothwell, Eds) *Introduction to Archaeological Sciences*, pp. 45–60. London: Wiley.

Grün, R. (2001*b*). ESR dose estimation on fossil tooth enamel by fitting the natural spectrum into the irradiated spectrum. *Rad. Meas.*, submitted.

Grün, R. & Brumby, S. (1994). The assessment of errors in the past radiation doses extrapolated from ESR/TL dose response data. *Rad. Meas.* **23,** 307–315.

Grün, R. & Macdonald, P. D. M. (1989). Non-linear fitting of TL/ESR dose response curves. *Applied Radiation and Isotopes* **40,** 1077–1080.

Grün, R., Beaumont, P. B. & Stringer, C. B. (1990). ESR dating evidence for early modern humans at Border Cave in South Africa. *Nature* **344,** 537–539.

Ikeya, M. (1993). *New Applications of Electron Spin Resonance: Dating, Dosimetry and Microscopy*. Singapore: World Scientific.

Kilburn, R. & Rippey, E. (1982). *Seashells of Southern Africa*. Johannesburg: Macmillan.

Martinson, D. G., Pisias, N G., Hays, J. D., Imbrie, J., Moore, T. C. & Shackleton, N. J. (1987). Age dating and the orbital theory of the ice ages: Development of a high-resolution 0 to 300,000-year chronostratigraphy. *Quatern. Res.* **27,** 1–29.

Miller, G. H. & Beaumont, P. B. (1989). Dating in the Middle Stone Age at Border Cave, South Africa, by the epimerization of isoleucine in ostrich egg shell. *Geol. Soc. Am., Abstracts with Programs* **21,** A235.

Miller, G. H., Beaumont, P. B., Deacon, H. J., Brooks, A. S., Hare, P. E. & Jull, A. J. T. (1999). Earliest

modern humans in southern Africa dated by isoleucine epimerization in ostrich eggshell. *Quatern. Sci. Rev.* **18,** 1537–1548.

Morris, A. G. (1992). Biological relationships between Upper Pleistocene and Holocene populations in southern Africa. In (G. Bräuer & F. H. Smith, Eds) *Continuity or Replacement. Controversies in Homo sapiens evolution*, pp. 131–143. Rotterdam: Balkema.

Nambi, K. S. V. & Aitken, M. J. (1986). Annual dose conversion factors for TL and ESR dating. *Archaeometry* **28,** 202–205.

Pearson, O. M. & Grine, F. E. (1996). Morphology of the Border Cave hominid ulna and humerus. *S. Afr. J. Sci.* **92,** 231–236.

Pfeiffer, S. & Zehr, M. K. (1996). A morphological and histological study of the human humerus from Border Cave. *J. hum. Evol.* **31,** 49–59.

Richards, D. (1981). *South African Shells: A collectors' guide*. Cape Town: Struik.

Rink, W. J. (1997). Electron spin resonance (ESR) dating and ESR applications in Quaternary science and archaeometry. *Rad. Meas.* **27,** 975–1025.

Robertson, S. & Grün, R. (2000). Dose determination on tooth enamel fragments from two human fossils. *Rad. Meas.* **32,** 773–779.

Shackleton, N. J., Berger, A. & Peltier, W. R. (1990). An alternative astonomical calibration of the lower Pleistocene timescale based on ODP Site 677. *Trans. R. Soc. Edinb.: Earth Sci.* **81,** 251–261.

Sillen, A. & Morris, A. G. (1996). Diagenesis of bone from Border Cave: implications for the age of the Border Cave hominids. *J. hum. Evol.* **31,** 499–506.

Simpson, J. J. & Grün, R. (1998). Non-destructive gamma spectrometric U-series dating. *Quatern. Sci. Rev.* **17,** 1009–1022.

Smith, F. H., Falsetti, A. B. & Donelly, S. M. (1989). Modern human origins. *Yearb. phys. Anthrop.* **32,** 35–68.

Vanhaelewyn, G., Callens, F. & Grün, R. (2000). EPR spectrum deconvolution and dose assessment of fossil tooth enamel using maximum likelihood common factor analysis. *Applied Radiation and Isotopes* **52,** 1317–1326.

Wintle, A. G. (1996). Archaeologically relevant dating techniques for the next century. Small, hot and identified by acronyms. *J. Archaeol. Sci.* **23,** 123–138.

Yang, Q. (1997). Experimental determination of beta attenuation in tooth enamel layers and its implication in ESR dating. Unpublished MSc Thesis, McMaster University, Hamilton.

Yang, Q., Rink, W. J. & Brennan, B. J. (1998). Experimental determinations of beta attenuation in planar dose geometry and application to ESR dating of tooth enamel. *Rad. Meas.* **29,** 663–671.

Yellen, J. E., Brooks, A. S., Cornelissen, E., Mehlman, M. J. & Stewart, K. (1995). A Middle Stone Age worked bone industry from Katanda, upper Semliki valley, Zaire. *Science* **268,** 553–556.